*Revised manuscript with no changes marked
Click here to view linked References

Modelling of hydrogen sulfide dispersion from the geothermal power plants of Tuscany (Italy)

Somma R.[1], Granieri D.[2], Troise C.[1], Terranova C.[1], De Natale G.[1], Pedone M.[1]

[1]*Istituto Nazionale di Geofisica e Vulcanologia Sez. Napoli Osservatorio Vesuviano Via Diocleziano, 328 - 80124 Napoli. Italy*

[2] *Istituto Nazionale di Geofisica e Vulcanologia Sez. Pisa Via Della Faggiola, 32 - 56126 Pisa. Italy*

Abstract

We applied the Eulerian code DISGAS (DISpersion of GAS) to investigate the dispersion of the hydrogen sulfide (H_2S) from 32 geothermal power plants (out of 35 active) belonging to the geothermal districts of Larderello, Travale-Radicondoli and Monte Amiata, in Tuscany (Italy). An updated geographic database, for use in a GIS environment, was realized in order to process input data required by the code and to handle the outputs. The results suggest that H_2S plumes emitted from geothermal power plants are mainly concentrated around the stacks of emission (H_2S concentration up to 1100 $\mu g/m^3$) and rapidly dilute along the dominant local wind direction. Although estimated values of air H_2S concentrations are orders of magnitude higher than in unpolluted areas, they do not indicate an immediate health risk for nearby communities, under the more frequent local atmospheric conditions. Starting from the estimated values, validated by measurements in the field, we make some considerations about the environmental impact of the H_2S emission in all the geothermal areas of the Tuscany region.

Keywords: hydrogen sulfide emissions, geothermal power plants, air quality, Tuscany region.

1. Introduction

One of the most important environmental issues related to the use of geothermal fluids to generate electricity is the emission of non-condensable gases to the atmosphere. Vent stacks from geothermal plants emit carbon dioxide (CO_2) and methane (CH_4) causing concern because of their role as greenhouse gases (Bloomfield and Moore, 1999; Bloomfield et al., 2003), despite those emissions are quite small compared to carbon and fossil fuel plants, indicating that the contribution of these sources is practically negligible (Miller and Van Atten, 2004). Geothermal power plants also emit hydrogen sulfide (H_2S) in relative high amounts (Peralta et al., 2013), since H_2S is one of the main constituents of the geothermal fluids, after H_2O and CO_2, and it is released into the atmosphere as waste pollutant of the entire productive cycle. The presence of H_2S in the air, and then in water, (Olafsdottir et al., 2014), soils and vegetation is one of the main environmental concerns for the areas that host geothermal fields.

The increase of geothermal energy production, and the consequent release of pollutants, such H_2S, has sometimes raised the opposition of the nearby living population, for example, at Puna, Hawaii (Anderson, 1991). The environmental impact, was also one of the reasons for which the population of Milos (Greece) obtained the stopping of geothermal energy production on the island (Marouli and Kaldellis, 2001). sulfideSome studies, in different geothermal districts, have been performed in order to evidence, at a sub-regional or local scale, the potential impacts on the environment of the H_2S and other trace elements (notably, mercury and arsenic) by the operation of geothermal power plants (Bargagli et al., 1986; Noorollahi Y, 1999; Bacci et al., 2000; Kristmannsdóttir et al., 2000; Loppi, 2001; Gurnasson et al., 2013; Peralta et al., 2013). Furthermore the H_2S toxicity for humans is a proven fact at certain concentrations (WHO, 2003), and the unpleasant odor, even at very low concentrations, can be detected far away from the emission points (Thorsteinsson et al., 2013).

In this study the dispersion into the atmosphere of the H_2S has been tested in order to evidence, via numerical code and GIS tools, coupled with field measurements, the possible impacts of the H_2S

emission on the inhabitants living close to the geothermal power plants belonging to the Tuscany geothermal districts. With this aim, we used a geomatic approach dedicated to data processing of geographic information necessary to run the code and to manage the outputs, and a mathematical approach, represented by the numerical code DISGAS (Costa et al., 2005; Granieri et al., 2013, 2014, 2015), for modelling the H_2S plume dispersion, starting from the stack emissions and the local meteorological conditions. The numerical code, we used, allows the definition of H_2S same-concentration lines, in the air, at different heights from the soil, representing a powerful instrument to identify the areas of the domain preferentially affected by the presence of H_2S, in function of the prevailing winds and hydrodynamic conditions of the atmosphere, and their values of concentrations. DISGAS code, moreover, could yield a reliable prediction of H_2S pollution in case of unexpected events, in view of the impact of future expansions of the geothermal energy production through new wells or new power plants.

2. Background

2.1. Features of the H_2S and effects on the human health

Hydrogen sulfide is a colorless water-soluble gas, with a characteristic odor of rotten eggs and defined for this putrid gas. Its origin may be natural, (about 90% of the total H_2S in the atmosphere, US Environmental Protection Agency, EPA, 1993) as gas species produced by anaerobic bacterial reduction of sulfur-containing animal and vegetable proteins and as gas released from volcanoes and geothermal areas (Aiuppa et al., 2005); but also anthropogenic, as product of industrial activities (Bates et al., 1992). The artificial origin of hydrogen sulfide derives from the production process of coking coal, cellulose (method with Kraft), fertilizers, dyes and pigments, refinement of crude petroleum, tanning of hides and skins, treatment of waste water.

Background concentrations of H_2S in ambient unpolluted air have been estimated to be between 0.14 and 0.4 $\mu g/m^3$ (US EPA, 1993), whilst the typical concentration in urban area is about one

order of magnitude higher (1.0-3.0 μg/m^3, Kurtidis et al., 2008). High air levels of H_2S are measured near waste-water treatment plants, oil refineries, and landfills (from a few units to a few tens of mg/m^3, WHO, 2003) as well as in volcanic and geothermal areas, where H_2S is likely formed by water-rock interaction, which is accelerated by the high heat gradient induced by the presence of a cooling magma body. In these environments, the H_2S is released in the atmosphere by hot vents and hot springs. In some sites of the quiescent Colli Albani volcano (Italy), Carapezza et al. (2012) found a H_2S air concentration >700 mg/m^3 which represents an immediately lethal value. Because H_2S is a gas, human exposure is principally via inhalation, and the gas is rapidly adsorbed through the lungs. Health effects include respiratory, ocular, neurological, and metabolic effects and the death after single exposures to concentrations ≥700 mg/m^3 (WHO, 2003). A summary of these effects is presented in Table 1 and hereafter discussed. H_2S is felt by humans at very low concentrations with a reference odor threshold equal to 0.011 mg/m^3 but becomes odorless at concentrations higher than 140 mg/m^3 (WHO, 2003) and, to values close to those lethal (≥700 mg/m^3) it has an odor almost pleasant. Inhalation of 2.8-14 mg/m^3 does not affect respiratory function in healthy men and women but lack of vigor, common ailments and states of agitation are common symptoms for elderly, young children and asthmatic individuals (WHO, 2003). In New Zealand, about 70% of workers exposed to daily concentrations than often exceeded 28 mg/m^3 complained of fatigue, loss of appetite, headaches, irritability, memory lapses, dizziness. At concentrations greater than 140 mg/m^3, olfactory paralysis occurs, causing a loss of odor perception; this makes H_2S very dangerous because one or two breaths at concentrations ≥700 mg/m^3 can be fatal (the so-called "slaughterhouse sledge-hammer" effect). Table 2 shows the allowable thresholds concentration in the air according to the guidelines of the World Health Organization (WHO) and regulations in the countries that cultivate geothermal fields (e.g., New Zealand and Iceland). In fact, the presence of H_2S is always verified in geothermal areas and in the vicinity of geothermal plants since H_2S is one of the main constituents of the geothermal fluid. In particular it can be released into the atmosphere from natural geothermal manifestations (fumaroles,

hot springs, geysers, soils degassing), as well as from conventional geothermal plants in case of exploitation of the underground resource as better explained in the following Section.

Soils may adsorb considerable amounts of H_2S from the air, retaining most of it as elemental sulfur (Cihacek and Bremner, 1993) but preferentially H_2S is oxidized by molecular oxygen and hydroxyl radicals of air (Davis et al., 1979), forming sulfur dioxide (SO_2) and ultimately sulfates (Hill, 1973), with a residence time in air typically less than 1 day. Sulfur dioxide and sulfates compounds are removed from the atmosphere through absorption by waters, plants and soils or through wet precipitation. The sulfur-containing compounds can cause fish deaths, while the effect on plants is related to a persistent removal of trace elements essential to the functioning of their enzymatic systems (Luther et al., 2004).

2.2. General functioning of a geothermal plant and geothermal plants in Tuscany

A geothermal power plant uses the hot pressurized fluid of the underground to generate electrical energy (DiPippo, 2016). The geothermal fluid is basically composed by dry steam or, more frequently by hot water and steam but always with a significant amount of gases and other compounds, notably CO_2, H_2S, CH_4, NH_3, Hg. The geothermal fluid may spontaneously reach the surface or, often, it remains confined within the reservoir because of the impervious covering. In such a case, the fluid can be extracted by means of wells (drilled to a depth of some kilometres). A single power plant can be fed by several geothermal wells. Hot, pressurized geothermal fluid is piped to the turbine (Fig. 1) where it rapidly expands and rotates turbine blades. Rotational energy from the turbine is converted to electrical energy through an alternator. Turbine and alternator represent the basic unit of the plant whose power defines the nominal power of the plant. From the turbine the steam is discharged to the condenser (Fig. 1) at a sub-atmospheric pressure (typically 0.08 bar). Inside the condenser, the water coming from the cooling tower is sprayed directly into the steam to enhance its condensation. Then, the mixture of cooling water and condensate is pumped to

the head of the cooling tower to extract the waste heat through an upward stream of cold air which actually becomes enriched in the gases of the natural fluid. An extractor provides to remove the non-condensable gases from the condenser, emitting them into the atmosphere. Any excess condensate, together with the tower blowdown, is reinjected into the reservoir (Fig. 1). The components of the power plant from which H_2S (and other gases) is emitted in the atmosphere are the cooling tower and primarily the extractor of non-condensable gas whose summed contributions define the total H_2S emission from the power plant.

The Italian geothermo-electrical generation is concentrated in Tuscany and thanks to this resource, Tuscany is the Italian region with the highest use of renewable sources. Geothermal energy covers, in fact, about 33% of the electricity needs in Tuscany (Razzano and Cei, 2015) and meets the electricity demand of about 2 million households (data from Enel Green Power, 2013).

Currently in Tuscany 35 geothermal power plants are operative (Fig. 2 and Table 3), which have a global nominal capacity of 914.5 MW (Razzano and Cei, 2015). Individual plants have nominal capacities ranging from 14.5 to 60 MW (Table 3). The 35 plants of the Tuscany (supplied by 235 wells) are controlled and operated from a remote control station located in Larderello (Pisa) by the Italian electrical energy company (ENEL Green Power). As shown in Fig. 2, the main geothermal districts are located in the Larderello area, in the Travale-Radicondoli area, and in the Monte Amiata area, this last including the geothermal fields of Piancastagnaio and Bagnore.

The geothermal area of Larderello (red symbols in Fig. 2) was the first in Italy and in the entire world used for the production of electricity (starting from 1913) and remains the most important geothermal field in Europe and among the first in the world (Bertani, 2016). The explored area is about 250 km^2, and has 200 wells producing about 4300 t/h of superheated steam at temperatures between 150-270 °C and pressures of 0.2-1.8 MPa, with an average content of non-condensable gas ranging from 1 to 15% by weight (Razzano and Cei, 2015). At present 22 plants are in operation in the district of Larderello, with a total nominal capacity of 594.5 MW (Table 3).

The geothermal field of Travale-Radicondoli (green symbols in Fig. 2) covers approximately 50 km^2, where 29 wells produce a total of 1300 t/h of superheated steam at 190-250 °C and 0.8-2 MPa pressure, with a content of non-condensable gas in the range 4-8% by weight (Razzano and Cei, 2015). In this area, 8 plants are in operation with a nominal capacity of 200 MW (Table 3). The condensate deriving from the exhaust steam is reinjected in the field of Larderello through a 20-km long piping system. The geothermal exploration, carried out during the 70s with numerous deep perforations, showed that Larderello and Travale-Radicondoli fields are connected to a unique, wide and deep (3000-4000 m) geothermal reservoir, with an extension of about 400 km^2 (Razzano and Cei, 2015).

The Monte Amiata geothermal district (yellow symbols in Fig. 2) includes the field of Piancastagnaio and Bagnore. They show a "water-dominated" system, at depth 2500-4000 m, with layer pressure of about 20 MPa and temperatures ranging from 300-350 °C. The non-condensable gas content ranges from 6 to 8% by weight (Razzano and Cei, 2015). There are currently 5 plants (2 in Bagnore and 3 in Piancastagnaio) with 120 MW of nominal capacity.

Most of the geothermal plants of Tuscany (29 out of 35, Table 3) are equipped with filters for the abatement of hydrogen sulfide and mercury, named AMIS® technology "Abbattimento Mercurio e Idrogeno Solforato" (Fig. 1). This technology has been developed and patented by ENEL (Baldacci et al, 2005), and allows an efficient removal of substances such as mercury and H_2S at the outlet of the extractor of non-condensable gases.

Other innovative technologies are employed in some plants of the Tuscany. The plant of Cornia 2 (Larderello area) is the first geothermal-biomass integrated power plant in the world, by 2015, equipped with a superheater boiler for geothermal steam and a combustion grate supplied by local forest woodchip, agricultural residues or special crops (Razzano and Cei, 2015). Furthermore, in 2013, was installed the first geothermal binary power plant in Italy as upgrade of Bagnore 3 (Monte Amiata district). This unit is fed by a secondary flash steam at low pressure which is obtained from

the partial evaporation for expansion of the liquid phase derived from the primary flash (Razzano and Cei, 2015).

3. Methods and data

3.1. Numerical Code

In order to model the dispersion into the air of the H_2S deriving from the geothermal power plants of Tuscany we applied the Eulerian DISGAS (DISpersion of GAS) code which is able to reproduce the passive dispersion in the atmosphere of a gaseous pollutant, released by point or diffuse sources. The code and the user's manual are freely available at http://datasim.ov.ingv.it/models/disgas.html and http://datasim.ov.ingv.it/download/disgas/manual-disgas-2.0.pdf, respectively (both accessed, Dec. 6, 2016).

DISGAS solves the equations of advection and diffusion of the gas in the event that the dispersion of the gas into the atmosphere is governed by wind and atmospheric turbulence (passive dispersion). The model treats the gas as inert and does not account for photo-oxidation in the atmosphere, wet precipitation or density, although the density of H_2S is higher than that of dry air. DISGAS is coupled with the pre-processor DWM (Diagnostic Wind Model, Douglas and Kessler, 1990), developed by the US EPA, that reproduces the kinematic effects of the morphology and soil-cover types on the local flow, i.e., lifting, acceleration, blocking effects due to terrain obstacles.

The inputs to the model include the topography and terrain roughness, location and emission rate of the pollutant source, meteorological data (in particular air temperature, barometric pressure and the wind field, calculated by DWM), atmospheric stability conditions (Monin-Obukhov length and friction velocity). The output of DISGAS consists in the generation of a 2D array (projected into an x-y referential plane, following the ground coordinates) of the gas concentrations, defined in the same domain of the topography and at different vertical layers.

To support the production of spatial input data for DISGAS, to simulate the dispersion of the H_2S and finally, to process the arrays of H_2S concentration, geographic multi-layer databases were created, for use in a GIS environment. In particular, it was necessary to use a Digital Terrain Model (DTM) with an appropriate resolution and a mapping of the roughness of the area covered by simulations through a reworking of the real soil use classes. Furthermore, multi-layer databases reporting the location of the geothermal power plants, air monitoring systems, meteorological stations, distribution of population centres have been developed.

3.2. Topography and roughness of the domains

The topographic data were acquired from TINITALY/01 DTM (Tarquini et al., 2007), with 10 m resolution in an x-y referential plane. This model was built using the coordinate reference in WGS84 UTM 32N for most of the territory of Italy and WGS84 UTM 33N only for Italian regions falling in zone 33. The topographic input also requires the indication of the roughness of the terrain that defines the mechanical interaction between the mass of air and the ground. The roughness must be defined in the same domain of the topography, even if the discretization of the region, i.e., the spacing of the grid in the x- and y-axis, can be different. The roughness values were defined with GIS procedures based on maps of land use. The model has been applied to three geographic domains, whose roughness maps are given in Appendix A (Figures A.1-A.4).

Larderello domain (Fig. A.1) extends over an area of about 17x16 km^2, that we subdivided into 1720x1596 cells (in the x and in the y direction, respectively) of 10 meters resolution.

Travale-Radicondoli domain (Fig. A.2) extends over an area of about 15x13 km^2, discretized using a grid square of 10 meters side with 1494 cells in the x direction and 1330 cells in the y direction.

Monte Amiata domain (Fig. A.3 and A.4) stretches over two areas (Piancastagnaio and Bagnore) of equal size, 9.5x8.5 km^2, we discretized using a grid square of 10 meters side with 935 cells in the x direction and 853 cells in the y direction.

The code is applied with 10 vertical layers (from 0 to 6 m above the ground) of increasing thickness between the surface and the top (Δz = 0.5 m and 1 m) to better highlight the gas concentration gradient near the ground. Unless otherwise stated, we mapped the H_2S concentrations at the height of 1.5 m; this being the typical breathing height of standing humans.

3.3. Meteorological data

Meteorological data including air temperature, barometric pressure and wind direction and speed were obtained from agro-meteorological stations managed by the Regional Hydrological Sector (SIR, "Settore Idrologico Regionale") of the Tuscany region (http://www.sir.toscana.it/). In detail, for Larderello district we considered the records from the "Castelnuovo Val di Cecina" station (056 code in the SIR of Tuscany); for Travale-Radicondoli district the "Pentolina" station (080 code in the SIR) and for Monte Amiata district (including Piancastagnaio and Bagnore areas) the "Piancastagnaio" station (080 code in the SIR). Table 4 shows, for each station considered, the main characteristics of wind dataset (direction of provenance, speed and acquisition time span). The employed datasets are of great significance as they are composed of some thousands of data, with daily frequency, over a large time span (from 5 years for Piancastagnaio station to 18 years for Pentolina station).

The wind provenance direction is clustered into 8 sectors of 45°, centered along a standard direction (N, NE and so on). Figure 3 shows the frequency of the wind occurrence over the acquisition period for each provenance sector, as also reported in Table 4.

In Larderello area, the more frequent winds blow from S and NE (Fig. 3, Castelnuovo Val di Cecina station) with intensity higher than for other areas (Table 4); in Travale-Radicondoli area, nearest to

Larderello district (Fig. 2), the prevailing winds are from NE and SW (Fig. 3 and Table 4, Pentolina station); instead, in Monte Amiata area a clearly prevailing wind from NW direction was recorded (Fig. 3 and Table 4, Piancastagnaio station).

We investigated the H_2S plume dispersion using the two more frequent wind conditions for each district, except for Monte Amiata where we used the wind from SE in the second step of simulations since it clearly blows toward the main inhabited centers of the area (see Section 4.4).

3.4. Atmospheric stability conditions

The atmospheric stability conditions are defined by the Monin-Obukhov length value (L, in m) (Monin and Obukhov, 1954). Lacking measurements of the turbulent component of the wind (obtainable through targeted micrometeorological campaigns) or measurements of the solar radiation or indications on cloud cover, necessary to calculate the value of L, we assumed unstable atmospheric conditions during the daytime (L= - 4.00 m from 9:00 am to 20:00 pm, local time) and stable conditions during the night (L = + 4.00 m from 21:00 pm to 8:00 am, local time). This indicating that the turbulence induced by the positive buoyancy of the air masses heated by solar radiation exceeds the mechanical mixing of the wind during the day (L negative). During the night, instead, the atmospheric condition is assumed inverted, therefore with low effects of turbulence and a tendency to stratification of air masses (L positive). These assumptions are consistent with the L theoretical values for daily cycles in non-coastal areas (Stull, 1988).

3.5. Emission rate of H_2S

The emission rates of H_2S can be accessed on the website of the Regional Environmental Protection Agency of Tuscany (ARPAT, http://www.arpat.toscana.it/documentazione/report/report-geotermia) that is in charge of monitoring the pollutant emissions from the geothermal power plants of the region.

In Table 5 we reported the more recent H_2S emission rates (expressed in kg/h) from 32 power plants (out of 35 active), located in Larderello, Travale-Radicondoli, and Monte Amiata geothermal districts. We assumed the total emission of H_2S for each plant, namely considering the gas output from the extractor of non-condensable gases and from the cooling tower, i.e., the so-called "central emission" reported in the ARPAT reports. For Nuova Lago and Nuova Serrazzano plants (Larderello district) data related to the H_2S emission rate have not been reported in the last years (at least from 2007), as well as for Bagnore 4 (operative by 2015) and then they have not been included in the simulated cases.

The amount of H_2S associated to the related plant is emitted into the model layer at 3.0 m above the ground.

4. Results

4.1. Calibration of the model

Considering the high degree of variability of the air movements and the large number of parameters involved in atmospheric processes, a model of dispersion of pollutant in air, however complex (high number of input parameters) and accurate (input data with negligible errors), will always provide a predicted output that differs from the observed data (Lamb, 1984). A good model and a proper calibration ensure that this difference is as small as possible.

In order to validate the model, simulated concentrations were compared with air H_2S concentrations measured by ARPAT in 2014 at the emission stacks of 8 geothermal plants in the Larderello area, during the usual activity of monitoring. Wind conditions assumed in this test are the two prevailing ones in Larderello area, i.e., wind from S and NE (intensity of 5.1 m/s and 4.4 m/s, respectively, see Table 4) and two others characterized by opposite wind directions, i.e., wind from N and SW (intensity of 4.2 m/s and 3.9 m/s, respectively, see Table 4); adopted hydrodynamic conditions of

the atmosphere are explained in Section 3.4 and H_2S emission rates from the power plants are reported in Table 6, together with measured and estimated H_2S concentrations.

The correlation with observation data is very satisfactory for all the conditions of wind (Fig. 4) and it gives confidence in the ability of the DISGAS code to reasonably reproduce the measured H_2S concentration in proximity of the gas source.

Other simulations were performed to test the results of the code at some distance from the gas source. They were based on meteorological parameters and air H_2S concentrations simultaneously collected between 14 and 27 March 2012 at a distance of about 2-3 km from the gas source, through a mobile station located in Piancastagnaio town. The set of measured parameters and their values are shown in Appendix B (Table B.1). In particular, we selected a 24-hour period (from 0:00 to 23:00 on March 19, 2012), characterized by high variability in the direction and intensity of the wind. On that day the prevailing wind blew from ESE with an occurrence of ~20% and an average speed of 1.44 m/s and from the WNW direction with an occurrence of ~8% and an average speed of 0.62 m/s. Winds from SE, WSW and SW were less common and less intense. We assumed the hydrodynamic conditions of the atmosphere explained in Section 3.4. The emission rates of H_2S from three geothermal power plants around the Piancastagnaio town (Piancastagnaio 3, Piancastagnaio 4 and Piancastagnaio 5) are reported in Table 6.

H_2S measurements were compared to predicted H_2S concentrations in the same place of the mobile station and at the same height above the ground (2 m). As general trend, the two series show higher values in a window of few hours in their early portions and then a common flattening for most of the considered timespan, with the exception of the steep peak in the late portion of the modeled series, probably for the inability of the code to reproduce the real situation in case of sudden and significant changes of the wind and the hydrodynamic conditions of the atmosphere. The correlation between the two signals increases if we forward-shift the modeled series by 5 hours (Fig. 5a), which could suggest a delay due to the time needed to the gas plume to reach the site of measurement, considering that the wind pushing the pollutant was weak and it wasn’t mainly addressed to the

measurement point. The cross-correlation procedure confirmed that the two signals reach a statistically significant fitting when the modeled series is forward shifted by 3-5 hours, with the highest degree of fit for a lag = +5h (Fig. 5b). The correlation plot between the 5h-shifted series and the measurements shows a satisfactory agreement (R^2= 0.90) along a fitting line with slope ~13 (Fig. 5c). The high slope of the linear regression (in an idealized condition the ratio between estimated and measured values should be 1:1, thus with slope = 1) evidences that the code overestimates the H_2S concentration at a distance from the gas source. This is not surprising since, as explained in Section 2.1, and supported by Olafsdottir et al. (2014), H_2S is rapidly oxidized in air, and oxidation is the largest sink estimated. In summary, the net H_2S amount which is measured a few kilometers downwind the power plants differs from the estimated amount due to a considerable loss of H_2S by progressive transformation of H_2S in other oxidized compounds along the plume transport pathway. Unfortunately, we had just a single checkpoint to verify the model, at distance from the source, although we believe that the significance is high considering its position in the domain and considering that the H_2S amount in the air decreases exponentially from the source, getting negligible at a distance of a few kilometers (Olafsdottir et al., 2014).

That said, we apply the reduction factor of 12.7 for all the outputs of the simulated cases, considering that the typical dimension of the simulation domain is of a few kilometers and nearby communities are located 3-4 km from the power plants. For instance, applying this “calibration” factor, a H_2S concentration of 1.95 ppb is estimated at the location of the mobile station of Piancastagnaio (Fig. 6), against a value of 24.74 ppb retrieved by the not-calibrated model; confirmed by a similar value of 2.58 ppb measured in the same point.

4.2. Model application in the Larderello district

The application of the code in the Larderello district was particularly complex because we considered the simultaneous emission of H_2S from 20 geothermal power plants. As said in Section

3.3, the code was applied for similar occurrences of the winds from S and NE and with H_2S emission rates reported in Table 5.

Figure 7 shows the maps of the air H_2S concentration at the height of humans inhalation (1.5 m from the ground), considering the provenance of the wind from S (Fig. 7a) and NE (Fig. 7b). Maximum values are estimated in the plume of Selva 1 and Carboli 1 and 2 plants, reaching values around 600 and 450 $\mu g/m^3$ for the two conditions of the wind. All these three plants are not equipped with AMIS® filters. Plumes are arranged with their major axis stretching along the considered wind directions and, in different ways, spread across the main towns of the area, located downwind of the plants. Considering the wind from S, with occurrence frequency around 35% (or 127 days/y), Larderello and Montecerboli towns are affected by air H_2S concentrations around 100 $\mu g/m^3$, while Castelnuovo Val di Cecina and Monterotondo are entirely H_2S-free (Fig. 7c). In the case of wind from NE (32% of occurrence, or 117 days/y) the towns are weakly (Castelnuovo Val di Cecina) or not at all (the other three ones) affected by the gas, as shown in Fig. 7d. In summary, the areas of the inhabited centers have H_2S concentrations in air below the threshold of concern for humans (150 $\mu g/m^3$ WHO, 2003), although large sectors of the domain have values higher than 7 $\mu g/m^3$ that is the threshold proposed by the WHO in order to avoid odor annoyance (WHO, 2003).

4.3. Model application in theTravale-Radicondoli district

For Travale-Radicondoli district, characterized by 8 geothermal power plants all equipped with AMIS® technology (Table 3), the code was applied for dominant wind directions from NE and SW (Table 4 and Figure 3, Pentolina station) and considering the H_2S emission rates of Table 5. Figures 8a and 8b represent the maps of the H_2S concentration at the height of 1.5 m from the ground level in that area. For both conditions of the wind, maximum concentrations were detected in the plume including the contribution of Travale 3 and 4 plants, with values up to 900 $\mu g/m^3$ for wind from NE and 1100 $\mu g/m^3$ for wind from SW (Fig. 8a and 8b, respectively). These two plants have a global

nominal power of 60 MW. Under the considered wind conditions, whose summed occurrence frequency is 52% (or about 190 days/y), towns and villages do not present alarming H_2S concentrations (Figures 8c and 8d) with the exception of the Montalcinello village that is mantled by H_2S concentrations higher than the allowable threshold when the wind blows from SW (Fig. 8d). Also in the Travale-Radicondoli area, as for Larderello, most of the domain lying downwind of the geothermal plants has H_2S concentrations higher than the nuisance threshold (Figures 8a and 8b).

4.4. Model application in the Monte Amiata district (Piancastagnaio and Bagnore areas)

For Monte Amiata district, the application of the numerical code resulted in considering the H_2S emission rates from 4 geothermal power plants out of 5 active (for Bagnore 4 plant, installed in 2014 and operative by 2015, no data of H_2S emissions are available, see Table 5). The local wind regime is characterized by a dominant circulation from NW with a frequency of occurrence of 64.6% (or 236 days/y), significantly higher than the other sectors (Table 4 and Figure 3, Piancastagnaio station). A first run of simulations was made assuming the dominant direction of the wind from NW (Fig. 9a), to which we have added the simulated case with wind from SE, since, although with low occurrence frequency (i.e., 3.4%), this condition it favorable to push the H_2S of the plants towards the main population centers of the area (Fig. 9b). Both simulations were made handling in a separate way the geographic area of Bagnore (with Bagnore 3 plant) and Piancastagnaio (with Piancastagnaio 3, 4, 5 plants). Figures 9a and 9b show the maps of H_2S concentrations at the height of 1.5 m from the ground level, after the merging of the areas. Estimated values are maximum in the plume including the contribution of Piancastagnaio 4 and 5 plants (up to 700 $\mu g/m^3$, Fig. 9a) when the wind blows from NW. In this very frequent condition, the main inhabited centers are not at all affected by H_2S, since they are upwind of the geothermal plants or off-center with respect to the main axis of the plume (Fig. 9a). In the case of wind from SE

the town of Piancastagnaio and Abbadia S. Salvatore (Piancastagnaio area) are mantled by the H_2S plume although with concentrations below the allowable threshold (Figures. 9b and 9c).

5. Discussion and conclusions

In the present study we applied a numerical code called DISGAS to model the dispersion of the H_2S emitted from geothermal power plants in the Tuscany region. To our knowledge, modeling dispersion of the geothermally-derived H_2S has not been done before in this region, although the activity of exploitation of the underground resource began here more than a century ago and H_2S represents a "waste" pollutant of the entire productive cycle. Something new is also the application of the code for a reducing species, such as the H_2S, unlike the previous applications of the code for oxidized volcanogenic gas, like CO_2 (Costa et al, 2005; Granieri et al., 2013, 2014) and SO_2 (Granieri et al., 2015). The first simulated scenario, starting from simultaneous measurements of atmospheric parameters and air H_2S concentrations, evidenced as the code overestimated the H_2S concentrations at some distance (2-3 km) outside the geothermal plants although with an overall good correlation with measurements (Fig. 5c). Interpretation of the data likely reflects the tendency of the H_2S to be oxidized in air after the output from the vent stacks. In the last decades several researches have been carried out to better understand the conversion of H_2S to SO_2 and sulfates in the atmosphere. Brown and Webster (1994) claim that oxidation of H_2S within aerosols is a slow process, but Cox and Sandalls (1974) concluded that photo-oxidation of H_2S to SO_2 is a major loss process for H_2S in the atmosphere.

Previous studies demonstrated that SO_2 is converted into H_2SO_4 and/or sulfate aerosol, proceeding by several processes as: (1) homogeneous SO_2-gasphase oxidation; (2) heterogeneous SO_2-oxidation in atmospheric droplets and on aerosol particles (Beilke and Gravenhorst, 1978), involving hydroxyl radical (Davis et al. 1979):

$$SO_2 + OH\cdot \rightarrow HOSO_2\cdot \qquad (1)$$

$HOSO_2\cdot + O_2 \rightarrow HO_2\cdot + SO_3$ (2)

$SO_3 + H_2O \rightarrow H_2SO_4$. (3)

Eq. (3) is a quasi-liquid phase reaction forming sulfuric acid in liquid-phase.

In a heterogeneous system in which gaseous SO_2 is in equilibrium with sulfur (IV)* in the aqueous phase, the following equations describe the equilibrium,

$SO_2 + H_2O \rightarrow SO_2\cdot H_2O$ (4)

$SO_2\cdot H_2O \rightarrow H^+ + HSO^{3-}$ (5)

$HSO^{3-} \rightarrow H^+ + SO^{3--}$ (6)

where $SO_2\cdot H_2O$ is physically-dissolved SO_2, HSO^{3-} is the bisulfite ion (formed by a very rapidly reaction, Beilke and Gravenhorst, 1978), and SO^{3--} is the sulfite ion.

Notice that these reactions (Eq. 1-6) lead to an increase of H^+ ions, as well as the same dissociation of the sulfuric acid. These processes lead to an increased acidification of the rains, the formation of which is catalyzed by the sulfate aerosols.

Furthermore, H_2S is highly soluble in water and will be actively washed out during heavy rainfall, or during high air humidity periods, accumulating on the soil as elemental sulfur (Cihacek and Bremner, 1993). These considerations strongly reflect the dependence of air H_2S concentrations on climatic factors, especially precipitation, air humidity, air temperature and wind regime (Olafsdottir and Gardarsson, 2013). For instance, minor or at least very slow conversion of H_2S to SO_2 is verified at the atmospheric conditions of Iceland (Kristmannsdóttir et al., 2000), but the same authors state that in a dry and sunny climate, the oxidation in atmosphere might lead to a great amount of H_2S being oxidized to SO_2. Our findings show a rapid reduction of the H_2S concentrations moving away from the emission points, likely reflecting a rapid oxidation of the H_2S at the weather conditions of the Tuscany.

The simulated scenarios, resulting from this work, consider the condition of the local prevailing wind, derived from the analysis of the records of wind direction and intensity of the last years (until 2013). Maximum estimated H_2S concentrations range from a few hundreds to more than 1000 $\mu g/m^3$ (Figures 7-9), but peaked values are probably more than an one order of magnitude higher in

correspondence of the vent stacks, considering that we applied a "reduction" precautionary factor of ~13 for all the simulated values for better fitting the H_2S concentrations measured at some distance from the sources. Following from that, we found the highest concentrations of H_2S in the plume of power plants devoid of filters for the abatement of H_2S (and Hg) in the fumes (AMIS® filters) or in case of power plants likely showing outdates technology. The former case is clearly evident in Larderello district, for Selva 1, and Carboli 1 and 2 power plants (Fig. 7a and 7b), the latter in Travale-Radicondoli district (Fig. 8a and 8b), notably for Travale 3 plant, whose H_2S emission is 66.1 kg/h (Table 5), an unusually high value considering the presence of the AMIS® filter and the capacity of the plant (20 MW as the majority of the considered geothermal plants, see Table 3). This simulated scenario can exceed the threshold value (150 $\mu g/m^3$ of H_2S) of human health protection in the nearby communities (Fig. 8d).

In general, no alarming situation has been noted for majority of communities located some kilometers from the power plants, in all the geothermal districts of the Tuscany (Larderello, Travale-Radicondoli and Monte Amiata). Rather, people could be in danger of being poisoned by H_2S just inside poorly-ventilated buildings (e.g., inside the power plant facilities), or in enclosed topographic locations in proximity of the emission points, when the stagnant atmospheric conditions (for example, during a quiet summer night) favor the persistence of the gas. This situation has been verified in volcanic environments for oxidized gas species (then more conservative in atmosphere than H_2S), such as CO_2 (Granieri et al., 2013; Carapezza et al. 2003, 2012; Beaubien et al., 2003) or SO_2 (Granieri et al., 2015) or for volcanogenic H_2S emitted by vents and soils with very elevated emission rates (e.g., in Colli Albani volcanic area, Carapezza et al., 2003, 2012; Beaubien et al., 2003) but it seems have a low probability of occurrence here, in consideration of the usual relatively low concentration of the gas in the plume. In fact, no lethal accidents involving humans have been reported in the geothermal areas of the Tuscany. Although insufficient studies exist with which to evaluate the health effects in human populations exposed for

long periods to low levels of H_2S (WHO, 2003) a truly common concern could be the very unpleasant odor of H_2S, even in very low concentrations, in particular to people not used to it, since most part of the sectors involved by the H_2S plume dispersion evidenced concentrations higher than the recommended threshold to avoid nuisance (7 $\mu g/m^3$).

Yet, great concerns could arise for the unusual large amounts of S, ultimately discharged in the environment. Moist soils may adsorb considerable amount of H_2S from the air, retaining most of it as elemental S (Cihacek and Bremner, 1993), and then acidifying. Sulfur dioxide and sulfate compounds, derived from the oxidation of the H_2S in the atmosphere, are eventually removed via absorption by plants and soils or via precipitation by soils (De Kok et al., 1991). From the soil, S-bearing compounds may reach the aquatic environment and may be transported because of their solubility. These sulfur-containing compounds can causes fish deaths, while the effect on plants is related to a persistent removal of trace elements essential to the functioning of their enzymatic systems. Furthermore, the high concentration of sulfur dioxide and sulfate compounds in the atmosphere can favor the acidification of rain.

These aspects, well known from a theoretical point of view, has been never adequately investigated in the geothermal districts of the Tuscany, at least for all we know. Rather, some studies focused on the environmental distribution of Hg in the geothermal area of Monte Amiata (Bargagli et al., 1986; Loppi S., 2001), evidenced a good correlation between Hg and S in lichens, used as bio-indicators, confirming the common geothermal origin for both compounds and their concentrations higher than background values in some investigated sites, like in the village of Aiole, nearest to Bagnore and Arcidosso town (Loppi S., 2001).

While the simulated scenarios here presented are consistent with the prevailing wind conditions and they estimate reasonable H_2S concentrations for each area, there are a number of possible improvements in the analysis. First, a better quantification of the loss of the emitted H_2S with the distance from the source, under the local meteorological conditions; second, more tightly spaced

checkpoints would be useful to constrain the model better. As to the first point, a photochemical module to apply to DISGAS is currently under way, thereby offering the possibility to determine the loss of H_2S for the process of oxidation in the atmosphere.

In general, the results here presented indicate the potential of DISGAS as a tool for an improved understanding of the atmospheric and environmental impacts of the H_2S continuous degassing from geothermal plants (baselines of the concentration level) but also its potential for reliable prediction of H_2S pollution in case of unexpected and impulsive events, like the blowout of a geothermal well or the malfunctioning of a geothermal plant resulting in an anomalous and not-controlled emission of gas in the atmosphere.

Appendices

Appendix A

In Appendix A the roughness maps of the investigated domains are shown (Figures A.1- A.4).

Appendix B

Meteorological parameters collected (in the period between 14 and 27 March 2012) through a mobile station in the Piancastagnaio town (Fig. 6) are given in Appendix B. In detail, measured meteorological parameters (wind direction, wind speed, air temperature and humidity, atmospheric pressure, and precipitations) are given in Tab. B.1. The station was also equipped with dedicated sensors to simultaneously measure the concentration of H_2S and particulate (PM10) in the air.
Moreover, data on March, 19 (from 0:00 to 23:00), highlighted in yellow, were used to calibrate the numerical code.

Acknowledgements

The research leading to these results has received funding from POR Toscana SIMPAS *POR* CREO FESR 2007-2013. Assistance and access to data from Dott. M. Desideri – Tuscany Region (SIRA)

Administration and the Tuscany Regional Environmental Agency (ARPAT) are also acknowledged. Pavlos Kassomenos (Director Associate Editor), and two anonymous reviewers are acknowledged for their constructive reviews. Finally, we acknowledged Karen Holmberg (New York University) for her help on improving the English.

References

Aiuppa, A., Inguaggiato, S., McGonigle, A.J.S., O'Dwyer, M., Oppenheimer, C., Padgett, M.J., Rouwet, D., Valenza, M., 2005. H_2S fluxes from Mt. Etna, Stromboli and Vulcano (Italy) and implications for the global volcanic sulfur budget. Geochim Cosmochim Acta. 69, 1861–1871. doi:10.1016/j.gca.2004.09.018.

Anderson I., 1991. Blowout blights future of Hawaii's geothermal power. New Sci. 1778:17

ARPAT, 2016. Tuscany Regional Agency for Environmental Protection (Agenzia Regionale Protezione Ambientale). Geothermal Reports. http://www.arpat.toscana.it/datiemappe/dati/concentrazioni-di-idrogeno-solforato-h2s-nelle-aree-geotermiche-della-toscana-anni-2011-2014.

Bacci, E., Gaggi, C., Lanzillotti, E., Ferrozzi, S., Valli, L., 2000. Geothermal power plants at Mt. Amiata (Tuscany-Italy): mercury and hydrogen sulfide deposition revealed by vegetation. Chemosphere. 40, 907-911.

Baldacci, A., Mannari, M., Sansone, F., 2005. Greening of Geothermal Power: An Innovative Technology for Abatement of Hydrogen Sulfide and Mercury Emission. Proceedings, World Geothermal Congress 2005, Antalya, Turkey, 24-29 April 2005, 5 pp.

Bargagli R., Barghigiani C. and Maserti B.E., 1986. Mercury in vegetation of the Mount Amiata area (Italy). Chemosphere. 15, 8, 1035-1042.

Bates, T.S., Lamb, B.K., Guenther, A. et al., 1992. J Atmos Chem. 14, 315. doi:10.1007/BF00115242

Beaubien, S.E., Ciotoli, G., Lombardi, S., 2003. Carbon dioxide and radon gas hazard in the Alban Hills area (central Italy) J. Volcanol. Geotherm. Res. 123, 63-80.

Beilke, S. and Gravenhorst G., 1978. Heterogeneous SO_2-oxidation in the droplet phase. Atmospheric Environment (1967). 12, 231-239. doi:10.1016/0004-6981(78)90203-2

Bertani, R., 2016. Geothermal power generation in the world 2010–2014 update report. Geothermics. 60, 31–43.

Bloomfield, K., Moore J. and Neilson, R., 2003. Geothermal Energy Reduces Greenhouse Gases. https://www.geothermal.org/PDFs/Articles/greenhousegases.pdf.

Bloomfield, K. and Moore, J., 1999. Geothermal Electrical Production CO_2 Emissions Study. www.inl.gov/technicalpublications/Documents/3314491.pdf.

Brown, K.L., Webster, J.G., 1994. H_2S oxidation in aerosols. In: Proceedings 15th PNOC-EDC Geothermal Conference, 37-44.

Carapezza, M.L., Barberi, F., Ranaldi, M., Ricci, T., Tarchini, L., Barrancos, J., Fischer, C., Granieri, D., Lucchetti, C., Melian, G., Perez, N., Tuccimei, P., Vogel, A., Weber, K., 2012. Hazardous gas emissions from the flanks of the quiescent Colli Albani volcano (Rome, Italy). Appl. Geochem. 27, 1767–1782.

Carapezza, M.L., Badalamenti, B., Cavarra, L., Scalzo, A., 2003. Gas hazard assessment in a densely inhabited area of Colli Albani volcano (Cava dei Selci, Roma). J. Volcanol. Geotherm. Res. 23, 81–94.

Cihacek, L.J., Bremner, J.M., 1993. Characterization of the sulfur retained by soils exposed to hydrogen sulfide. Communications in Soil Science and Plant Analysis. 24, 85–92.

Costa, A., Macedonio, G., Chiodini, G., 2005. Numerical model of gas dispersion emitted from volcanic sources. Annals of Geophysics. 48, 805-815.

Cox, R.A., Sandalls, F.J., 1974. The photo-oxidation of hydrogen sulfide and dimethyl sulfide in air. Atmospheric Environment. 8, 1269-1281.

Davis D.D., Ravishankara A.R. and Fischer S., 1979. SO_2 Oxidation via the hydroxyl radical atmospheric fate of HSO_x radicals. Geophysical Research Letters. 6, 113-116.

De Kok, L.J., Rennenberg, H., Kuiper, P.J.C., 1991. The internal resistance in spinach leaves to atmospheric hydrogen sulfide deposition is determined by metabolic processes. Plant Physiology and Biochemistry. 29, 463–470.

DiPippo R., 2016. Geothermal power plants : principles, applications, case studies, and environmental impact. Butterworth-Heinemann is an imprint of Elsevier Elsevier pp. 742

Douglas, S., and R. Kessler (1990), User's Manual for the Diagnostic Wind Model, edited by Carr, L. (San Rafael, CA), vol. III, EPA-450/4-90-007C.

ENEL Green Power, 2013.
https://www.enelgreenpower.com/en-gb/plants/renewable_energy/geothermal

Granieri, D., Costa, A., Macedonio, G., Bisson, M., Chiodini, G., 2013. Carbon dioxide in the urban area of Naples: contribution and effects of the volcanic source. J. Volcanol. Geotherm. Res. 260, 52–61.

Granieri, D., Carapezza, M.L., Barberi, F., Ranaldi, M., Ricci, T., and Tarchini L., 2014. Atmospheric dispersion of natural carbon dioxide emissions on Vulcano Island, Italy. J. Geophys. Res. Solid Earth. 119. doi:10.1002/2013JB010688.

Granieri, D., Salerno, G., Liuzzo, M., La Spina, A., Giuffrida, G., Caltabiano, T., Giudice, G., Gutierrez, E., Montalvo, F., Burton, M.R., Papale, P., 2015. Emission of gas and atmospheric dispersion of SO_2 during the December 2013 eruption at San Miguel volcano (El Salvador, Central America). Geophys. Res. Lett. 42, 5847-5854, ISSN: 1944-8007. doi:10.1002/2015GL064660.

Gunnarsson, I., Arodottir, E.S., Sigfusson, B., Gunnlaugsson, E., Juliusson, B.M., 2013. Geothermal Gases Emission from Hellisheiddi and Nesjavellier Power Plant, Iceland GCR Transaction. 37, 785-789.

Hill, F.B., 1973. Atmospheric sulfur and its links to the biota. Brook-haven Symposia in Biology. 30, 159–181.

Kristmannsdóttir, H., Sigurgeirsson, M., Ármannsson, H., Hjartanson, H., Ólafsson, M., 2000. Sulfur gas emissions from geothermal power plants in Iceland. Geothermics. 29, 529–538.

Kurtidis, K., Kelesis, A., Petrakaskis, M., 2008. Hydrogen sulfide (H_2S) in urban ambient air. Atmospheric Environment. 42, 7476-7482.

Lamb, R.G., 1984. Air pollution models as descriptors of cause-effect relationships. Atmos Environ. 18, 591-606.

Loppi, S., 2001. Environmental distribution of mercury and other trace elements in the geothermal area of Bagnore (Mt. Amiata, Italy) Chemosphere. 45, 991-995.

Luther, G.W., Ma, S., Trouwborst, R. et al., 2004. Estuaries. 27, 551. doi:10.1007/BF02803546

Marouli, C., Kaldellis, J.K., 2001. Risk in the Greek electricity production sector. Proc. 7Th International conf. environ. Sci. technol. Ermoupolis, Syros Island, Greece, Sept. 2001, 305-314.

Miller, P.J., Van Atten, C., 2004. Emisiones atmosféricas de las centrales eléctricas de América del Norte. Comisión para la Cooperación Ambiental para América del Norte, Montreal, Canada http://www.cec.org/.

Monin, A.S.; Obukhov, A.M.,1954. Basic laws of turbulent mixing in the surface layer of the atmosphere. Tr. Akad. Nauk SSSR Geofiz. Inst. 24, 163–187.

Noorollahi, Y., 1999. H_2S and CO_2 dispersion modelling for the Mesjavellir geothermal power plant, S-Iceland and preliminary geothermal environmental impact assessment for the Theistareykir

area, NE-Iceland Reports Number 10 Geothermal training programme Orkustonfnun, Grensasvegru 9, IS-108 Reykiavik, Iceland 1999. pp. 247-284.

Olafsdottir, S., Gardarsson, S.M., Andradottir, H.O., 2014. Natural near field sinks of hydrogen sulfide from two geothermal power plants in Iceland. Atmospheric Environment. 96, 236-244.

Olafsdottir S., Gardarsson S.M., 2013. Impacts of meteorological factors on hydrogen sulfide concentration downwind of geothermal power plants. Atmospheric Environment. 77, 185-192.

Peralta, O., Castroa,T., Durónb, M., Salcidoc, A., Celada-Murilloc, A,T,, Navarro-González, R., Márqueza, C., Garcíaa, J., De la Rosad, J., Torresa, R., Villegas-Martínezc, R., Carreón-Sierrac, S,, Imaze, M., Martínez-Arroyoa, A., Saavedraa, I., De la Luz Espinosaa, M., Torres-Jaramillof, A., 2013. H_2S emissions from Cerro Prieto geothermal power plant, Mexico, and air pollutants measurements in the area. Geothermics. 46, 55-65.

Razzano, F., and Cei, M., 2015. Geothermal Power Generation in Italy 2010-2014 Update Report, Proceedings World Geothermal Congress 2015, Melbourne, Australia, 19-25 April 2015.

Stull, R.B., 1988. An Introduction to Boundary Layer Meteorology. Kluwer Academic Publishers, Dordrecht, The Netherlands. pp 667.

Tarquini, S., Isola, I., Favalli, M., Mazzarini, F., Bisson, M., Pareschi, M.T., Boschi E., 2007. TINITALY/01: a new Triangular Irregular Network of Italy. Annals of Geophysics. 50, 407-425.

Thorsteinsson, T., Hackenbruch, J., Sveinbjörnsson, E., Jóhannsson, T., 2013. Statistical assessment and modelling of the effects of weather conditions on H_2S plume dispersal from Icelandic geothermal power plants. Geothermics. 45, 31–40.

US EPA, 1993. Report to Congress on hydrogen sulfide air emissions associated with the extraction of oil and natural gas. ResearchTriangle Park, NC, US Environmental Protection Agency, Office of Air Quality Planning and Standards EPA/453/R93045; NTIS Publication No. PB9413122.

World Health Organization (WHO), 2003. Hydrogen Sulfide: human health aspects, Concise International Chemical Assessment Document n. 53, 35 pp, Geneva, Switzerland. www.who.int/ipcs/publications/cicad/en/cicad53.pdf.

Figure captions

Figure 1 - Simplified scheme of a standard geothermal power plant equipped with AMIS® technology (from Baldacci et al., 2005). Red squares: features the three fundamental steps of the AMIS® process: 1) removal of mercury by chemical absorption; 2) selective catalytic oxidation of hydrogen sulfide to SO_2; 3) SO_2 scrubbing by geothermal water.

Figure 2 - Location and extent of the geothermal areas of Tuscany. In red symbols: Larderello; in green Travale/Radicondoli; and yellow: Mt. Amiata power plants. Centered circles are power plants equipped with AMIS® filters. Circles: power plants without AMIS® filters. Triangles are the weather station used for the simulation. In pink shadow are the main urbanised areas.

Figure 3 - Frequency of wind occurrence (in %) according to the provenance direction for three weather stations of Tuscany. See text.

Figure 4 - Measured and estimated H_2S concentrations in air in proximity of the stack emissions of the geothermal plants. For each measured value there are four estimated values since we performed simulation cases assuming winds from S, NE, N, and SW.

Figure 5 - a) Comparison between H_2S concentration modeled series and measurements. The +5h shifted modeled series is also reported; b) Cross-correlation between modeled series and measurements for lags ranging from -12 to +12 h; c) Dispersion plot between estimated values (after the +5 h shift) and measurements (falling in the gray area of the diagram in a).

Figure 6 - Average map of H_2S concentrations in the air, under the wind conditions recorded on March 19, 2012. The red star indicates the position of the mobile station in the small Piancastagnaio town (grey area), which has acquired the meteorological parameters (including wind speed and

direction) and the H_2S concentration in the air. The rose diagram shows the distribution of the wind direction on that day.

Figure 7 - Maps of the H_2S concentration in the air, at 1.5 m above the ground, in the Larderello district assuming a) wind blowing from S and b) wind from NE; in c) and d) are shown the H_2S concentrations along the A-B-C cross-section passing through the main inhabited centers of the area (red dashed line drawn both in a) and b)). The value of 150 $\mu g/m^3$ has been proposed by the World Health Organization as the threshold limit for the protection of human health (WHO, 2003), while 7 $\mu g/m^3$ is the threshold to avoid odor annoyance (WHO, 2003).

Figure 8 - Maps of the H_2S concentration in the air, at 1.5 m above the ground, in the Travale-Radicondoli district assuming a) wind blowing from NE and b) wind from SW; c) H_2S concentrations along the cross-section A-B drawn in a); d) H_2S concentrations along the cross-section A-B-C drawn in b); A-B and A-B-C (red dashed lines) pass through the main inhabited centers of the area. The threshold for the protection of humans (isoline of 150 $\mu g/m^3$) and the threshold to avoid odor annoyance (isoline of 7 $\mu g/m^3$) are also reported.

Figure 9 - Maps of the H_2S concentration in the air, at 1.5 m above the ground, in the Monte Amiata district (Bagnore and Piancastagnaio areas) assuming a) wind blowing from NW and b) wind from SE; c) H_2S concentrations along the cross-section A-B (red dashed line) drawn in b) passing through two main inhabited centers of the area. The threshold for the protection of humans (isoline for 150 $\mu g/m^3$) and the threshold to avoid odor annoyance (isoline for 7 $\mu g/m^3$) are also reported.

Table 1

Click here to download Table: Table 1.docx

Table 1 - Human health effects resulting from exposure to H_2S (WHO, 2003)

Exposure (mg/m^3)	**Effect / observation**
0.011	Odour threshold (geometric mean but depending on the individual)
2.8	Bronchial constriction in asthmatic individuals
5.0	Increased eye complaints
7.0-14.0	Increased blood lactate concentration, decreased skeletal muscle citrate synthase activity, decreased oxygen uptake
5.0-29.0	Eye irritation
28.0	Fatigue, loss of appetite, headache, irritability, poor memory, dizziness
>140	Olfactory paralysis
>560	Respiratory distress
≥700	Death

Table2
Click here to download Table: Table 2.docx

Table 2 - Maximum permissible H_2S concentrations in the air on recommendations of the World Health Organization (WHO) and various national regulations.

Country/Agency	Level ($\mu g/m^3$)	Period average exposure
WHO[a]	150 100 20 7	Average over 24h 1-14 days Up to 90 days Average over 30 min. To avoid odour annoyance
Iceland[b]	50	Average over 24h (the limit may be exceeded 5 times per year). From 1st July 2014 the limit may not be exceeded
New Zeland[c]	7	Average over 1h (limit based on odour nuisance)
US EPA California[d]	43	Average over 1h

[a] WHO, 2003, Hydrogen Sulfide: Human Health Aspects, World Health Organization, Geneva, 2003
[b] Regulation 514/2010, Annex 1. http://www.government.is.
[c] Ministry for the Environment of New Zealand 2002. Ambient air quality guidelines. 2002 Update.
[d] United States Environmental Protection Agency (US EPA), California, Air Resources Board 1984: Sulfide ambient air quality standard.

Table3
Click here to download Table: Table 3.docx

Table 3 - Geothermal power plants in Tuscany on 31 December 2014 (data from the report of the Tuscany Regional Agency for Environmental Protection, ARPAT, 2015. http://www.arpat.toscana.it/documentazione/report/report-geotermia/monitoraggio-delle-aree-geotermiche-toscane-anno-2014, accessed Sept. 6, 2016).

Geothermal district	Name of power plant	Year of commissioning	Nominal power (MW)	AMIS Filter (Y=yes N=no)
Larderello	Carboli 1	1998	20	N
	Carboli 2	1997	20	N
	Cornia 2 [a]	1994	20	N
	Farinello	1995	60	Y
	Le Prata	1996	20	Y
	Monteverdi 1	1997	20	N
	Monteverdi 2	1997	20	N
	Nuova Castelnuovo	2000	14.5	Y
	Nuova Gabbro	2002	20	Y
	Nuova Lago	2002	10	Y
	Nuova Lagoni Rossi	2009	20	Y
	Nuova Larderello	2005	20	Y
	Nuova Molinetto	2002	20	Y
	Nuova Monterotondo	2002	10	Y
	Nuova San Martino	2005	40	Y
	Nuova Sasso	1996	20	Y
	Nuova Serrazzano	2002	60	Y
	Sasso 2	2009	20	Y
	Selva 1	1997	20	N
	Sesta 1	2002	20	Y
	Vallesecolo Gruppo 1	1991	60	Y
	Vallesecolo Gruppo 2	1992	60	Y
Subtotal	**22 plants**		**594.5**	**Y=16 N=6**
Travale-Radicondoli	Chiusdino 1	2010	20	Y
	Nuova Radicondoli 1	2002	40	Y
	Nuova Radicondoli 2	2010	20	Y
	Pianacce	1987	20	Y
	Rancia 1	1986	20	Y
	Rancia 2	1988	20	Y
	Travale 3	2000	20	Y
	Travale 4	2002	40	Y
Subtotal	**8 plants**		**200**	**Y=8 N=0**
Monte Amiata	Bagnore 3 [b]	1998	20	Y
	Bagnore 4 [c]	2014	40	Y
	Piancastagnaio 3	1990	20	Y
	Piancastagnaio 4	1991	20	Y
	Piancastagnaio 5	1991	20	Y
Subtotal	**5 plants**		**120**	**Y=5 N=0**
Total	**35 plants**		**914.5**	**Y=29 N=6**

[a]Geothermal-biomass combined power plant from 2015 (Razzano and Cei, 2015)
[b]Upgraded to binary power plant in 2013 (Razzano and Cei, 2015)

[c]Two new 20 MW units have been installed in 2014 and operative by 2015 (Razzano and Cei, 2015)

Table 4
Click here to download Table: Table 4.docx

Table 4 - Wind conditions at three meteorological stations of Tuscany[a].

Name of the station	Dataset period (daily series)	Wind provenance (Dir.)[b]	Wind frequency (%)	Wind speed (m/s)
Castelnuovo Val di Cecina (Larderello area)	03-10-2002 30-09-2013	N	7.5	4.2
		NE	32.0	4.4
		E	1.4	3.3
		SE	4.0	5.0
		S	34.8	5.1
		SW	17.3	3.9
		W	1.9	2.9
		NW	1.1	3.0
Pentolina (Travale-Radicondoli area)	05-05-1995 30-09-2013	N	3.0	1.8
		NE	27.0	1.6
		E	8.6	1.2
		SE	2.5	1.9
		S	15.6	2.2
		SW	24.9	1.6
		W	7.7	1.9
		NW	10.6	1.4
Piancastagnaio Monte Amiata (Piancastagnaio and Bagnore areas)	16-04-2008 30-09-2013	N	2.2	2.1
		NE	2.2	1.5
		E	1.4	0.8
		SE	3.4	1.4
		S	14.0	1.8
		SW	3.2	1.6
		W	8.9	1.2
		NW	64.6	1.2

[a]Data from the "Settore Idrologico Regionale" of the Tuscany region (http://www.sir.toscana.it/, accessed Sept. 6, 2016)
[b]Wind direction is clustered into 8 sectors of 45°, each of them centered along a "standard" direction (e.g, wind centered on N includes winds coming from the sector 367.5°-22.5°, wind centered on NE includes winds coming from the sector 22.5°-67.5°, and so on)

Table 5
Click here to download Table: Table 5.docx

Table 5 - H_2S emission rates from the power plants considered in the simulated cases.

Geothermal District	Name of power plant	H_2S emission (kg/h)[a]	ARPAT Sampling date[a]
Larderello	Carboli 1	13	Mar. 2013
	Carboli 2	46	Jul. 2014
	Cornia 2	34.6	Nov. 2014
	Farinello	11	Mar. 2012
	Le Prata	17.7	May 2014
	Monteverdi 1	11.1	Jul. 2013
	Monteverdi 2	23.7	Jul. 2013
	Nuova Castelnuovo	9.3	Mar. 2014
	Nuova Gabbro	12.7	May 2014
	Nuova Lagoni Rossi	13.2	Jun. 2013
	Nuova Larderello	9	Nov. 2014
	Nuova Molinetto	37.1	Aug. 2013
	Nuova Monterotondo	8.6	2010
	Nuova San Martino	6	Nov. 2013
	Nuova Sasso	12.3	Jun. 2013
	Sasso 2	4.8	Jun. 2013
	Selva 1	88	Mar. 2014
	Sesta 1	13.8	Aug. 2013
	Vallesecolo Gruppo 1	13.6	Oct. 2014
	Vallesecolo Gruppo 2	9	May 2012
Subtotal	**20 plants**		
Travale-Radicondoli	Chiusdino 1	28.9	Apr. 2014
	Nuova Radicondoli 1	2.7	Sep. 2014
	Nuova Radicondoli 2	7.8	Sep. 2014
	Pianacce	17.9	2011
	Rancia 1	7	Feb. 2014
	Rancia 2	7	Feb. 2014
	Travale 3	66.1	Oct. 2013
	Travale 4	28.4	Oct. 2013
Subtotal	**8 plants**		
Monte Amiata	Bagnore 3	7.8	Nov. 2014
	Piancastagnaio 3	9.6	Sep. 2014
	Piancastagnaio 4	23	Sep. 2014
	Piancastagnaio 5	14.7	Oct. 2014
Subtotal	**4 plants**		
Total	**32 plants**		

[a]Total emission from the power plant considering the gas output from the extractor(s) of non-condensable gases and from the cooling tower(s). Data from the annual reports of ARPAT (http://www.arpat.toscana.it/documentazione/report/report-geotermia and http://www.arpat.toscana.it/documentazione/report/report-geotermia/monitoraggio-delle-aree-geotermiche-toscane-anno-2014, accessed Sept. 6, 2016)

Table 6
Click here to download Table: Table 6.docx

Table 6 - Measured and estimated H_2S concentrations (using two wind directions) in 8 geothermal plants of Larderello district.

Name of power plant	ARPAT monitoring date[b]	H_2S emission (kg/h)[b]	H_2S measured conc. (mg/m^3)[b]	H_2S estimated conc. (mg/m^3)[c]	H_2S estimated conc. (mg/m^3)[d]
Carboli 2[a]	Jul. 2014	46	11.4	13.7	11.1
Cornia 2[a]	Nov.2014	34.6	10.2	10.7	8.8
Le Prata	May 2014	17.7	3.4	6.2	4.7
Nuova Castelnuovo	Mar. 2014	11.1	2.8	2.9	2.3
Nuova Gabbro	May 2014	23.7	2.0	5.2	3.2
Nuova Larderello	Nov.2014	9.3	2.2	4.2	2.3
Selva 1[a]	Mar. 2014	12.7	19.0	27.2	22.0
Vallesecolo Gruppo 1	Oct. 2014	13.2	1.0	4.2	3.4

[a]Power plant without AMIS filters
[b]Data are accessed at http://www.arpat.toscana.it/datiemappe/dati/emissioni-di-acido-solfidrico-h2s-degli-impianti-geotermici-anni-2010-2014, accessed Sept. 6, 2016
[c]Wind from the S
[d]Wind from the NE

Figure 1

Click here to download high resolution image

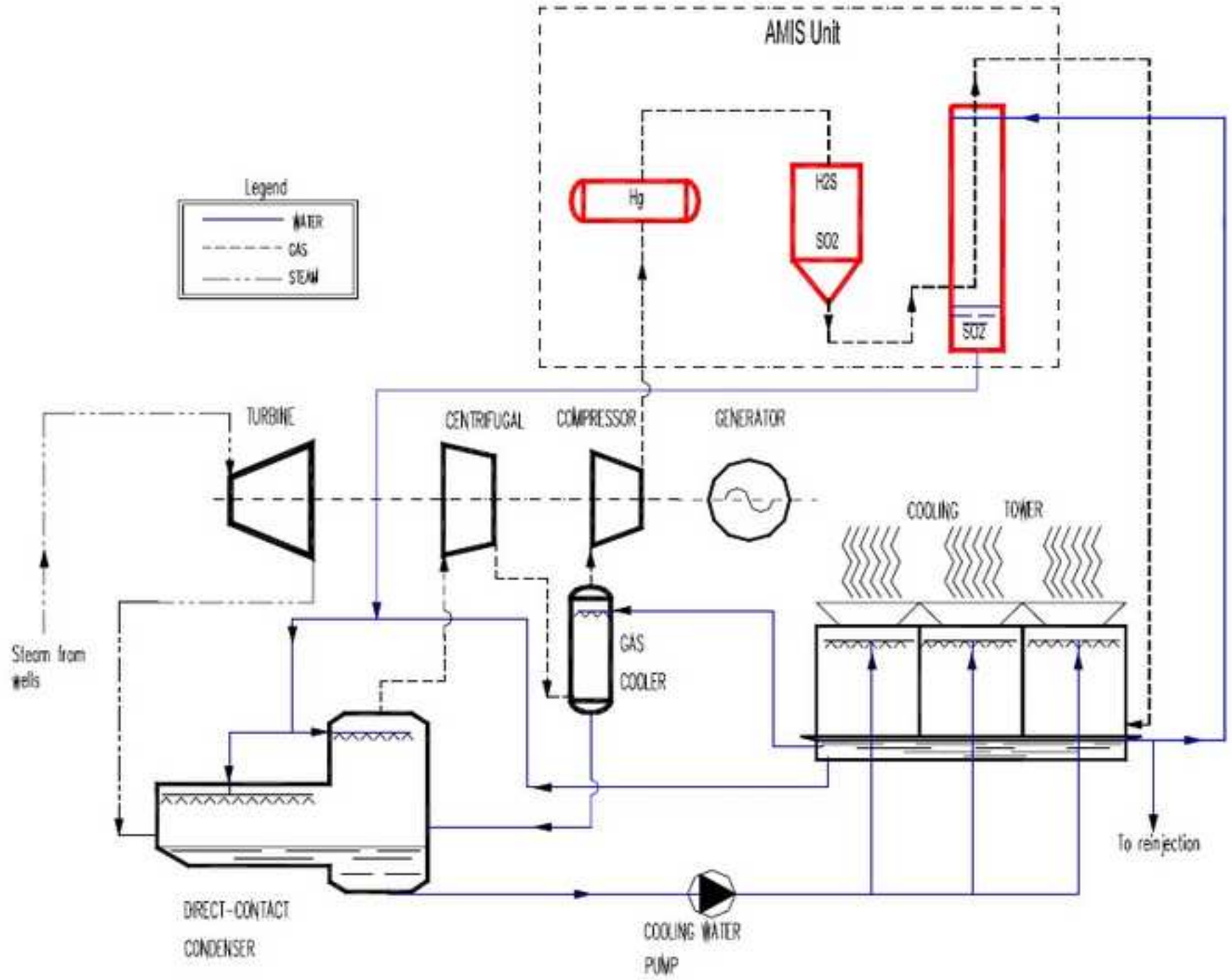

Figure 2

Click here to download high resolution image

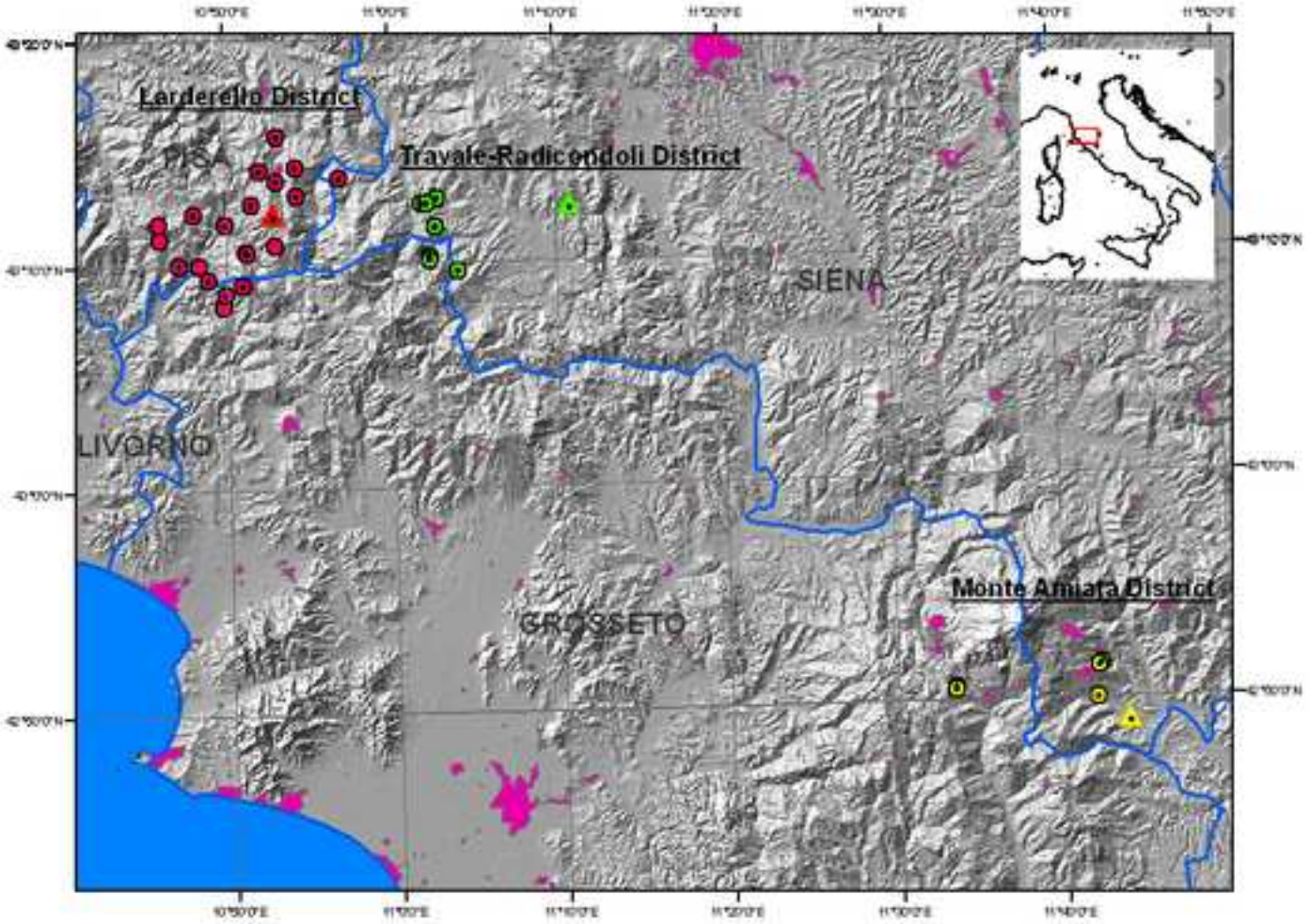

Figure 3

Click here to download high resolution image

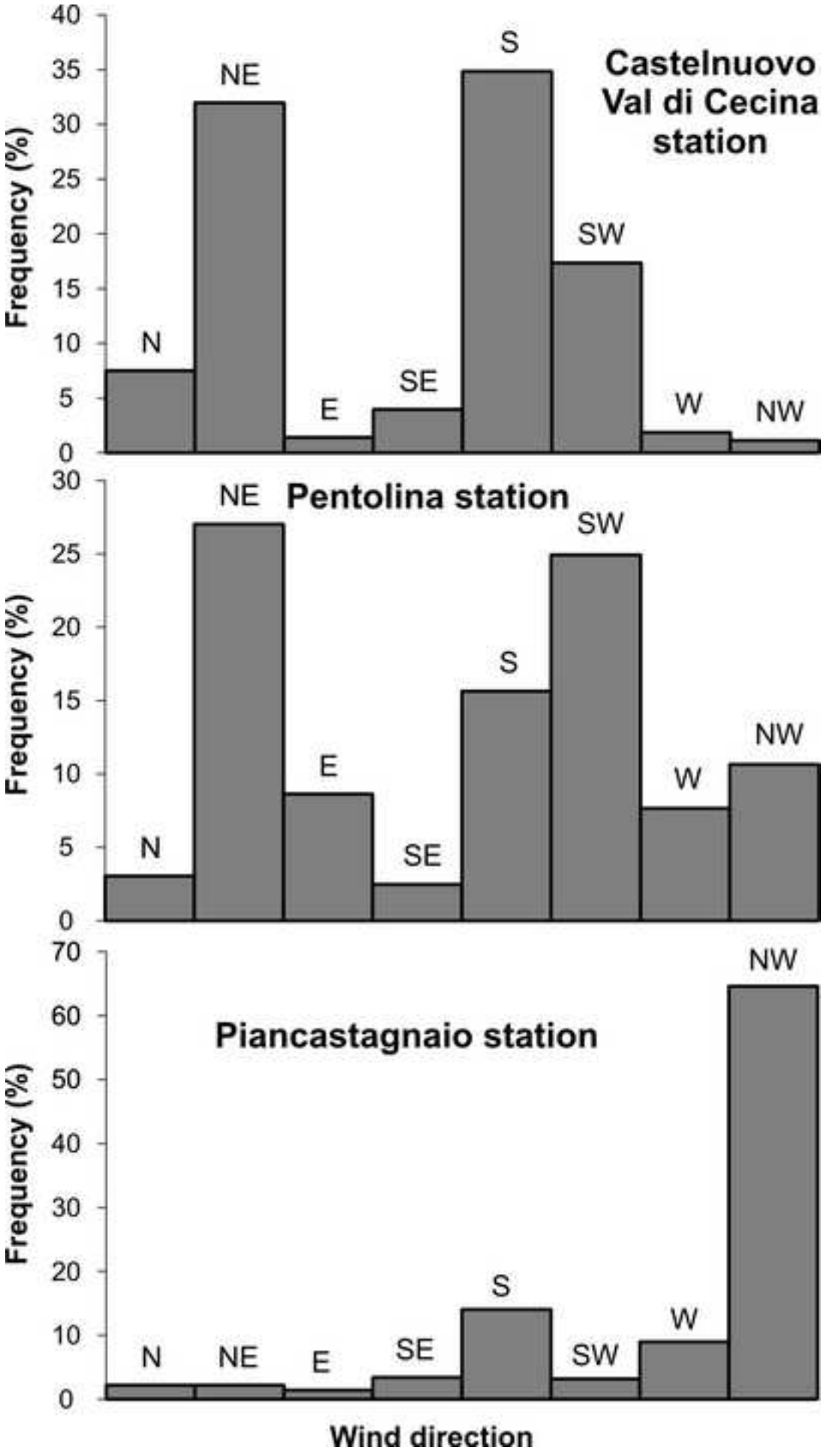

Figure 4

Click here to download high resolution image

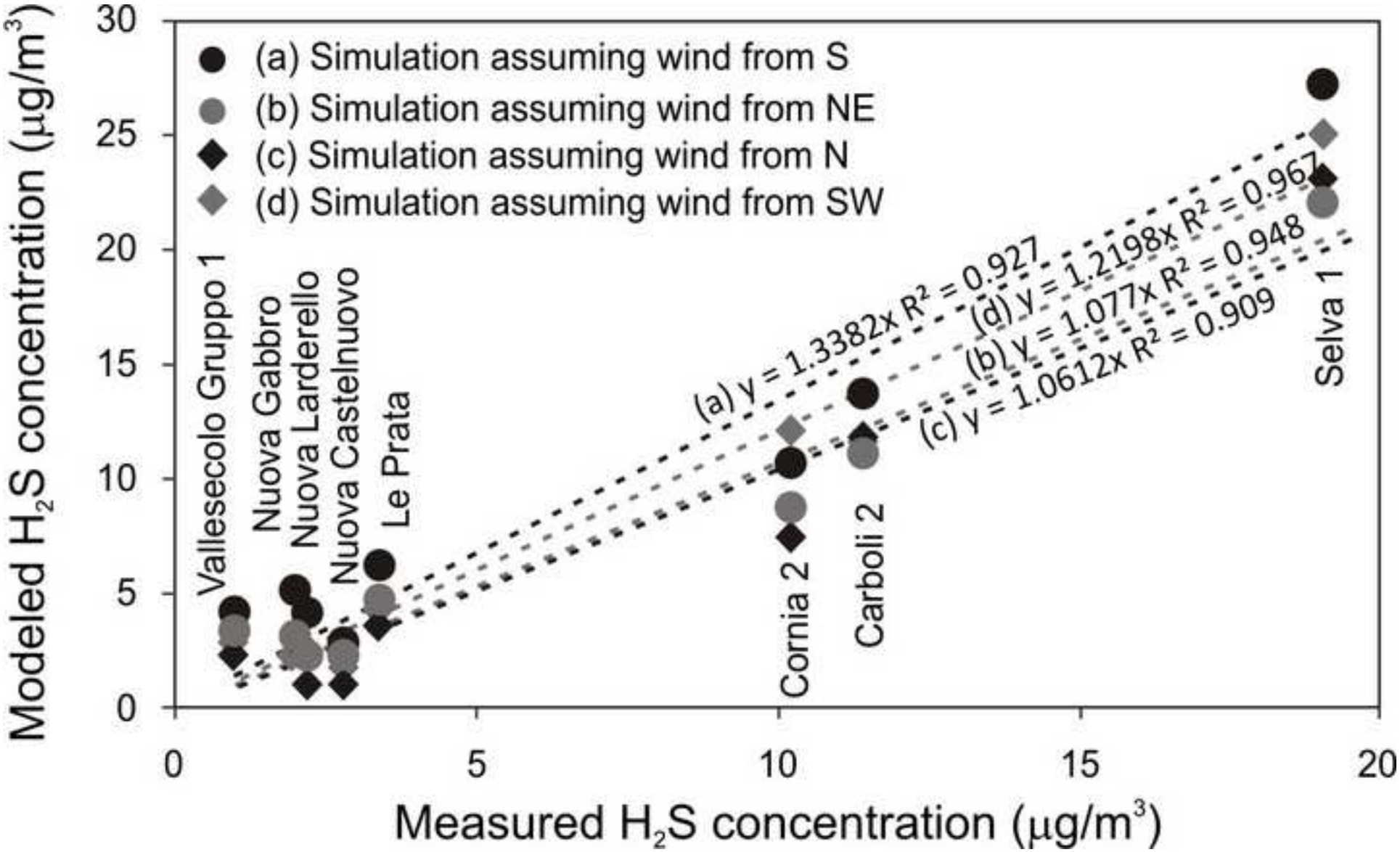

Figure 5

Click here to download high resolution image

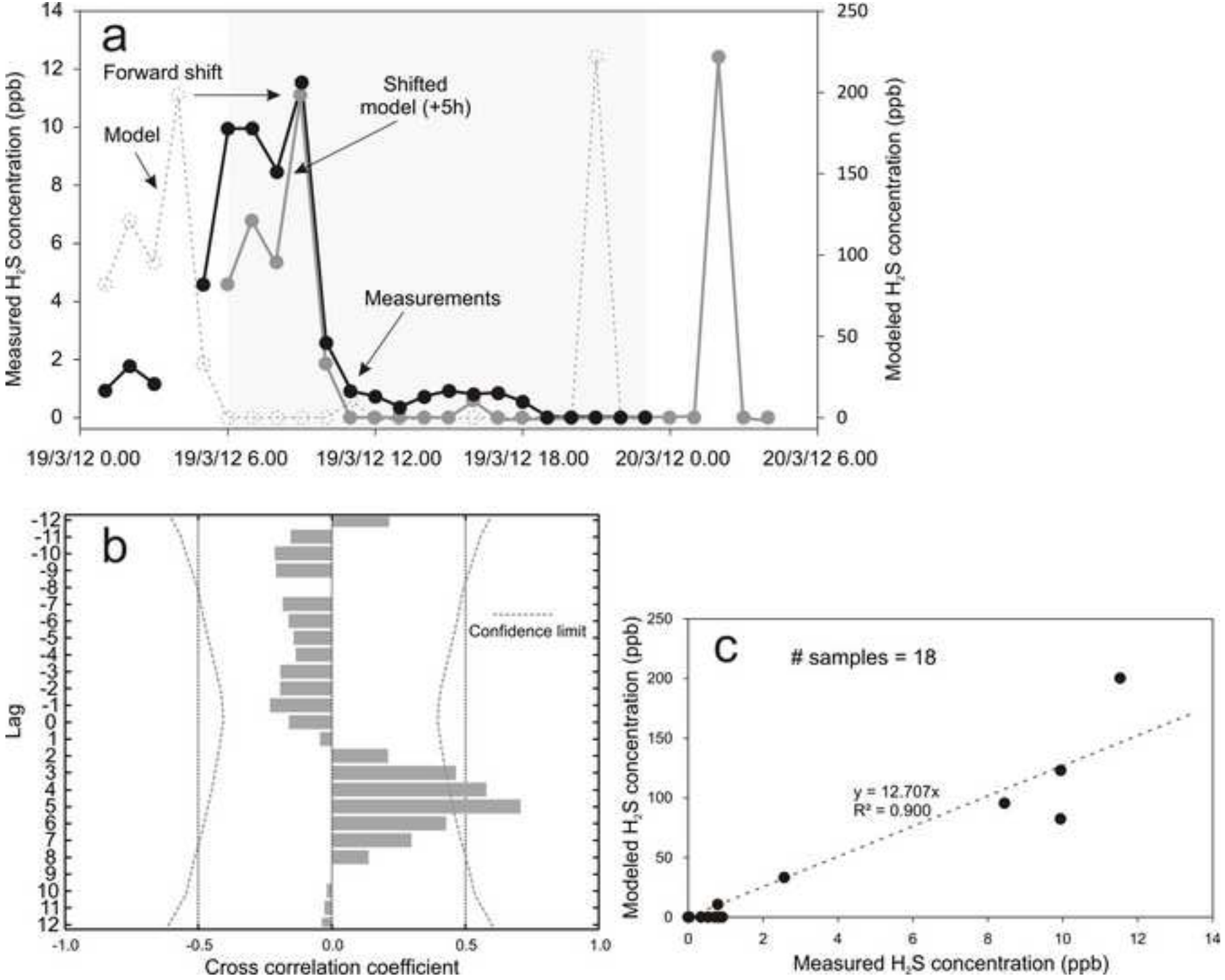

Figure 6

Click here to download high resolution image

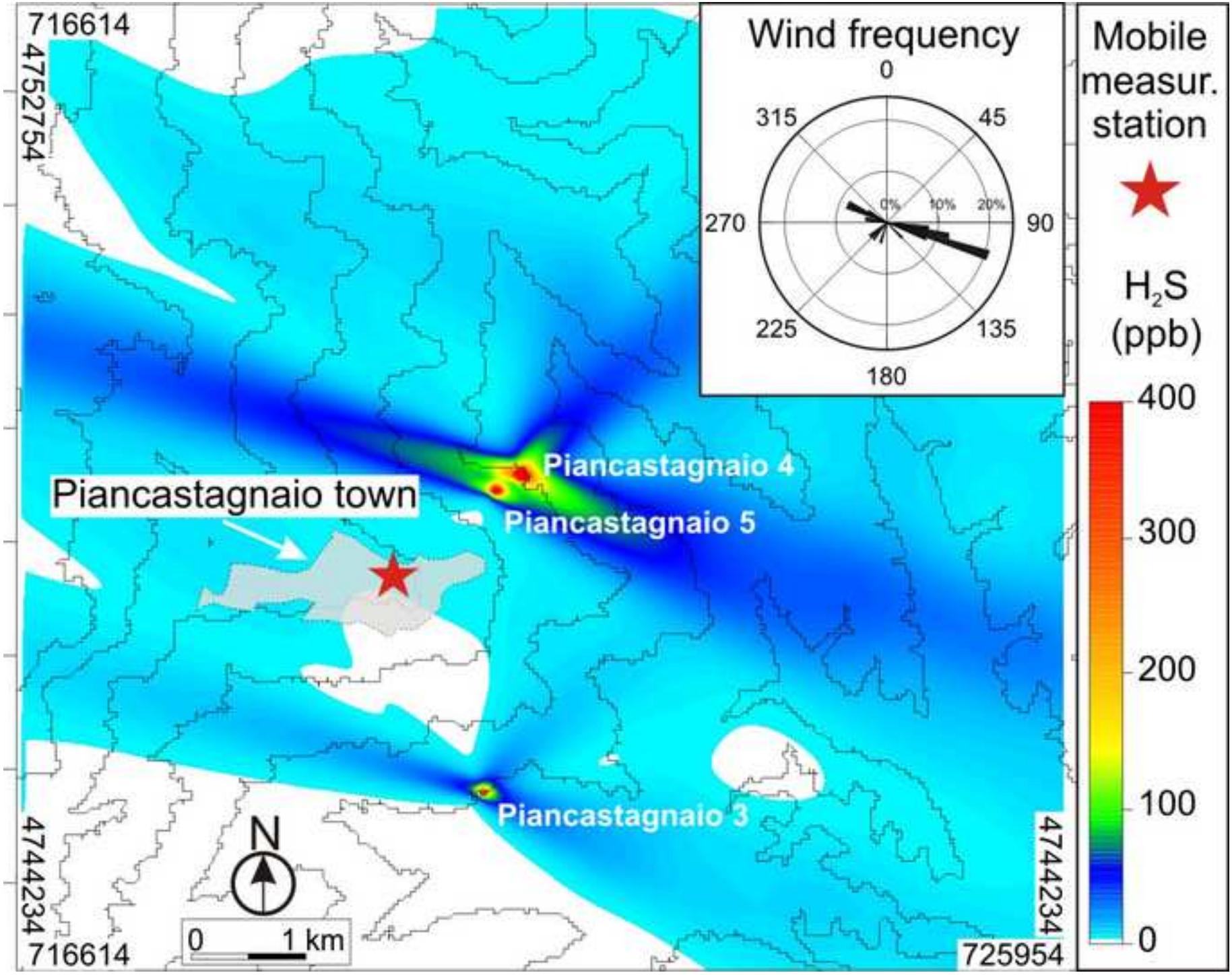

Figure 7

Click here to download high resolution image

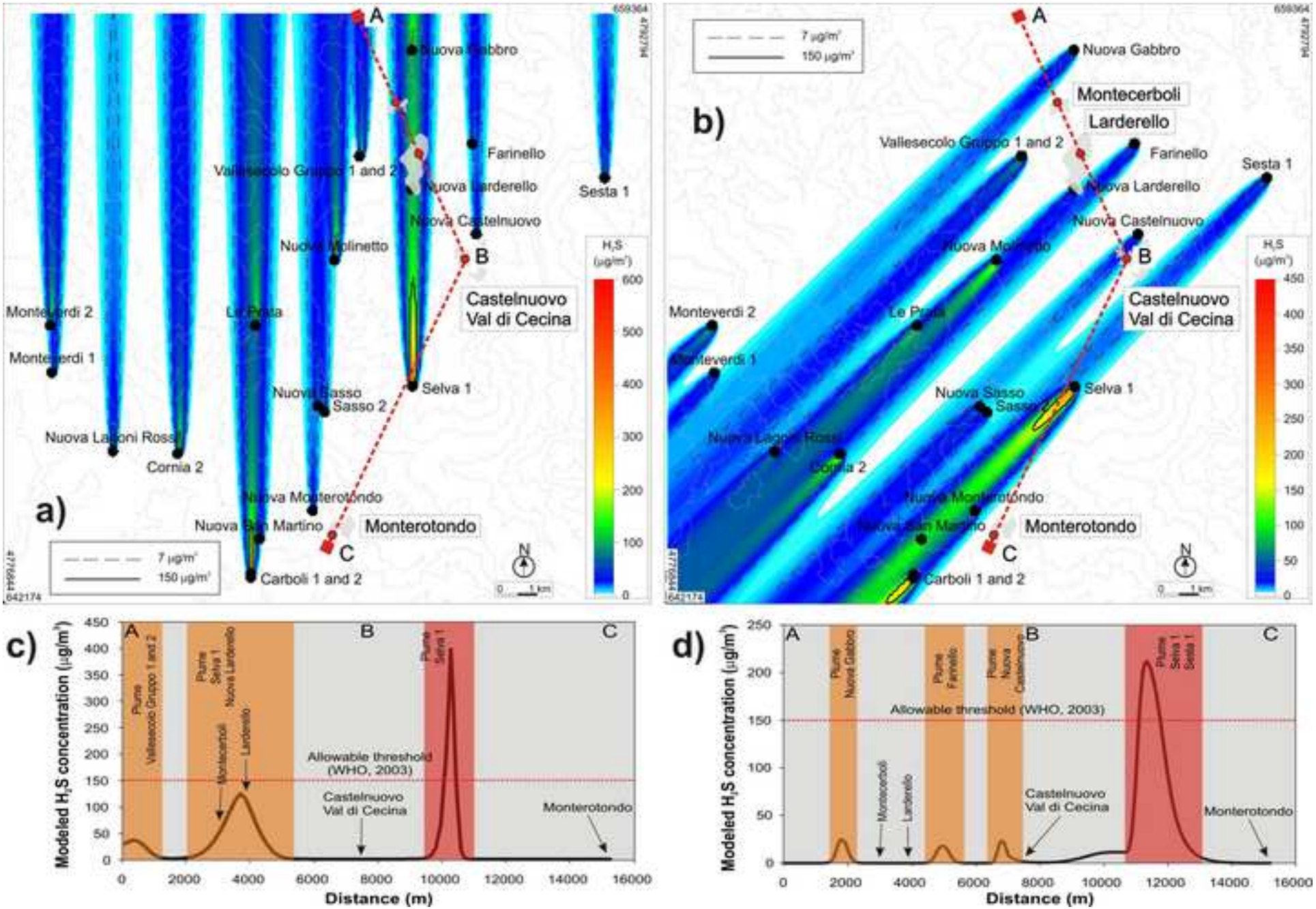

Figure 8

Click here to download high resolution image

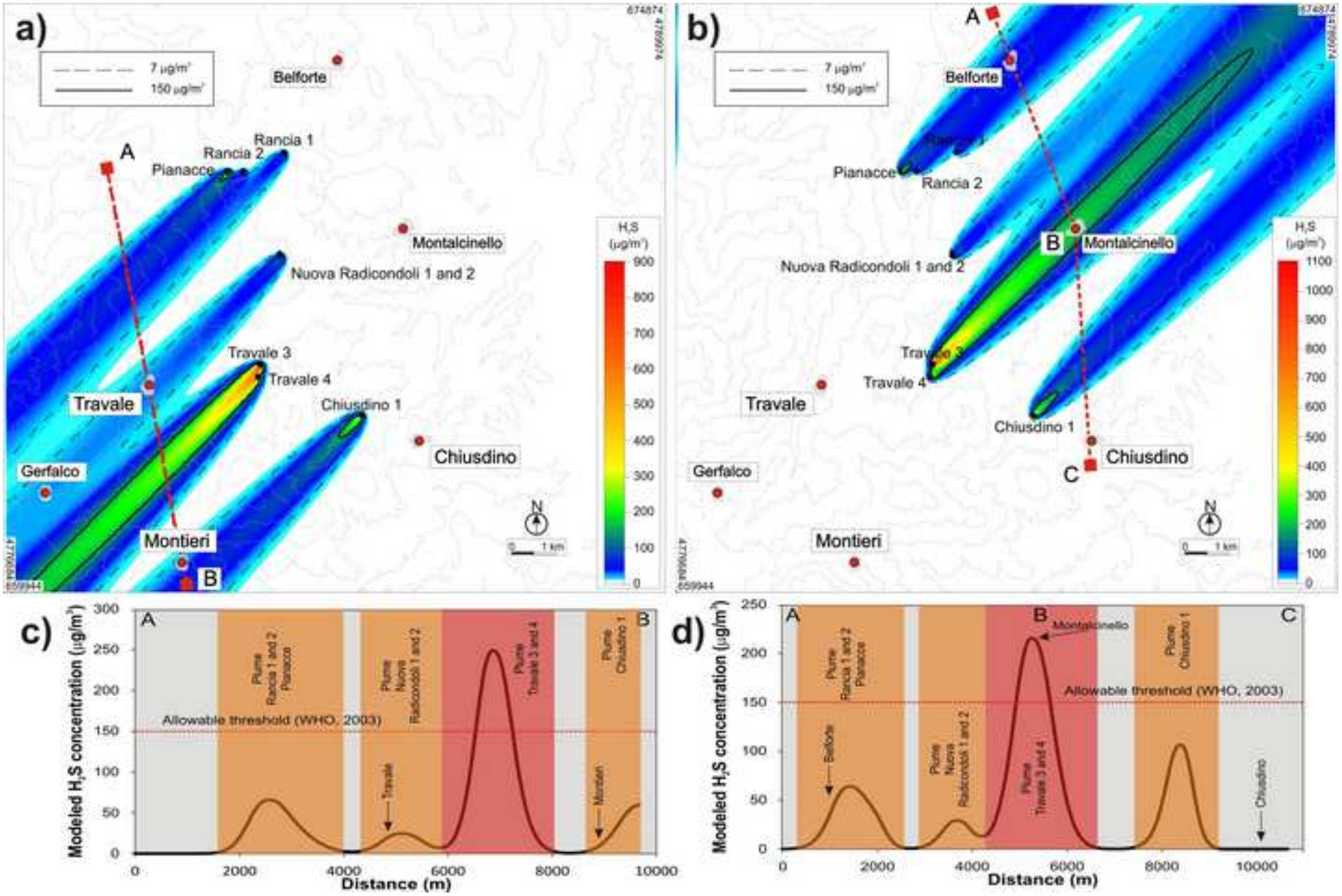

Figure 9

Click here to download high resolution image